Current Biology 22, 862–871, May 22, 2012 ©2012 Elsevier Ltd All rights reserved DOI 10.1016/j.cub.2012.03.059

Article

NR5A Nuclear Receptor Hr39 Controls Three-Cell Secretory Unit Formation in *Drosophila* Female Reproductive Glands

Jianjun Sun[1] and Allan C. Spradling[1,*]
[1]Howard Hughes Medical Institute Research Laboratories, Department of Embryology, Carnegie Institution for Science, 3520 San Martin Dr., Baltimore, MD 21218, USA

Summary

Background: Secretions within the adult female reproductive tract mediate sperm survival, storage, activation, and selection. *Drosophila* female reproductive gland secretory cells reside within the adult spermathecae and parovaria, but their development remains poorly characterized.
Results: With cell-lineage tracing, we found that precursor cells downregulate *lozenge* and divide stereotypically to generate three-cell secretory units during pupal development. The NR5A-class nuclear hormone receptor Hr39 is essential for precursor cell division and secretory unit formation. Moreover, ectopic Hr39 in multiple tissues generates reproductive gland-like primordia. Rarely, in male genital discs these primordia can develop into sperm-filled testicular spermathecae.
Conclusion: *Drosophila* spermathecae provide a powerful model for studying gland development. *Hr39* functions as a master regulator of a program that may have been conserved throughout animal evolution for the production of female reproductive glands and other secretory tissues.

Introduction

In species where fertilization takes place internally, including mammals and insects, the penetration of an egg only culminates a sperm's long and obstacle-filled journey through the female reproductive tract. Prior to reaching its target, both paternal [1] and maternal [2–4] reproductive tissues deploy mechanisms that strongly influence an individual sperm's chances for success. In particular, specialized glands in female reproductive tracts produce mucus-rich secretions that capacitate sperm to fertilize successfully, inhibit infection, and provide nutritional, maintenance, and storage factors. The interactions of sperm and seminal fluid with the female reproductive tract and its secretions in *Drosophila* offer an opportunity to genetically analyze these complex processes [3, 5–7].

Two paired glands, spermathecae (SPs) and parovaria (POs), are the primary sources of secretions encountered by sperm within the *Drosophila* female reproductive tract (Figure 1A). Messenger RNAs (mRNAs) encoding serine proteases, serpins, antioxidants, immune proteins, and enzymes involved in mucus production are found in SPs [5, 8–10]. Whereas two SPs arise from the *engrailed*$^-$ (*en*$^-$) and *en*$^+$ domains of the A8 segment, both POs originate in the *en*$^+$ domain of the A9 segment in the female genital disc during pupal development (Figures 1B and 1C) [11, 12]. Both types of mature gland contain large, polyploid secretory cells (SCs). Each SC connects with the gland lumen via a specialized cuticular canal equipped with a secretion-collecting "end apparatus" (Figure 1D) [13]. Anatomically related secretory units are found in SPs from other species [14] and in insect epidermal glands that produce pheromones, venoms, and many other products [15, 16]. Despite their ubiquity, insect epidermal gland development has not been well characterized at the molecular genetic level.

Studies of genital disc development and patterning [17, 18] have identified multiple genes important for reproductive gland formation. *lozenge (lz)*, encoding a runt-domain transcription factor, is essential for both SP and PO formation [19] and may be directly regulated by the sex determination pathway [20]. Homologous to mammalian AML-1, Lz also supports developing blood precursors and prepatterns ommatidial cells in the developing eye [21]. The *dachshund (dac)* gene also acts in multiple imaginal discs and is specifically needed for spermathecal duct development [22]. Mutations that disrupt sphingolipid metabolism [23] also cause abnormalities in spermathecal number and structure.

One of the most interesting genes needed to form reproductive glands encodes the nuclear hormone receptor Hr39, an early ecdysone-response gene [5, 24]. Hr39 and Ftz-f1 are the only two NR5A class nuclear hormone receptors in *Drosophila*, a class that in mammals includes steroidogenic factor 1 (SF-1) and liver receptor homolog 1 (LRH-1). All four of these proteins share 60%–90% sequence identity within their DNA binding domains and bind in vitro to identical sequences. SF-1 is a master regulator of steroidogenesis and sex hormone production [25], whereas LRH-1 is required in the ovary for female fertility [26], in embryonic stem cells for pluripotency [27, 28] and in endodermal tissues for metabolic homeostasis [29, 30]. Weak *Hr39* mutations alter the production of some SP gene products [5], whereas LRH-1 directly controls major secretory proteins of the exocrine pancreas [31]. Thus, NR5A class hormone receptors may play a conserved role controlling secretions from certain tissues, including female reproductive glands.

Here, we characterize the cell lineage of developing reproductive glands and clarify the roles of *lz* and *Hr39*. *Hr39* is expressed sex-specifically in *lz*-positive female gland primordia beginning shortly after the ecdysone pulse that initiates prepupal development. When levels of *Hr39* are reduced, *lz*-expressing precursors fail to protrude, divide, or remain viable, suggesting that *Hr39* expression orchestrates reproductive gland development. Mouse *LRH-1*, but not *SF-1*, can partially replace *Hr39* function in gland formation. Ectopic expression of *Hr39* in male larvae can induce a pigmented SP-like structure containing sperm to develop in the male reproductive tract. We propose that Hr39 acts as a master regulator of reproductive gland development and that the production of sperm-interacting proteins in the female reproductive tract under the control of NR5A proteins has been conserved during evolution. These findings suggest new targets for controlling agriculture pests and human-disease vectors.

*Correspondence: spradling@ciwemb.edu

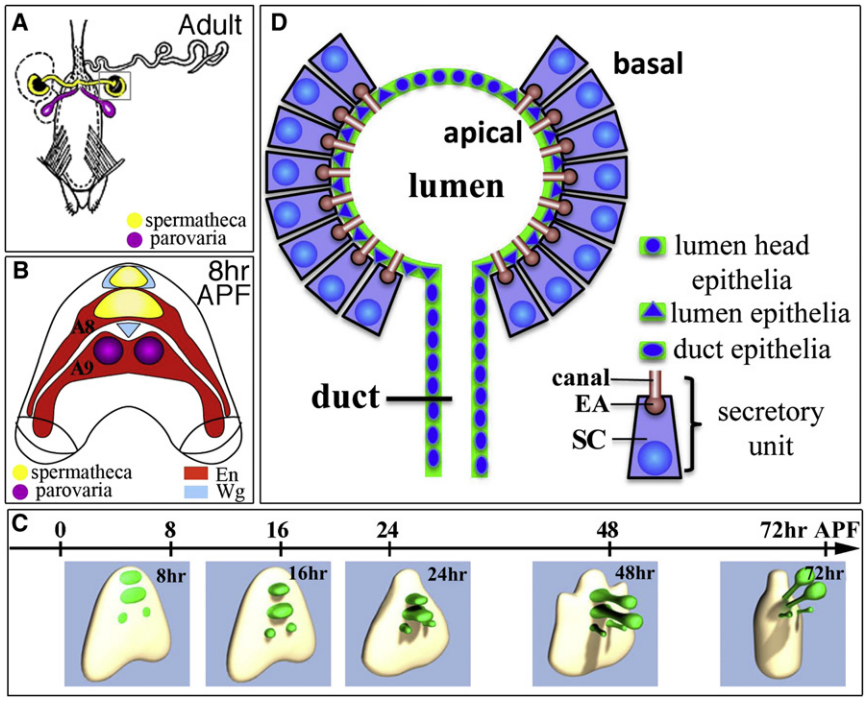

Figure 1. Structure and Origin of *Drosophila* Female Reproductive Glands

(A) Diagram of the female lower reproductive tract showing the paired SPs (yellow) and POs (purple).

(B) Diagram of the dorsal view of an early pupal genital disc (8 hr APF) showing the location of SP and PO primordia relative to zones of En and Wg expression in the A8 and A9 segments.

(C) Time course of reproductive gland (green) protrusion and morphogenesis during pupation. Diagrams show dorsal-lateral view of the genital discs.

(D) Diagram showing a SP in cross-section revealing the duct and the gland lumen, lined by chitin, underlying epithelial cells (green) and numerous secretory units consisting of a gland cell (purple) connected to the lumen by a chitinous canal (tan). Gland cell secretions are released via abundant microvilli into an "end apparatus" (EA), a specialized collecting zone of the canal.

Results

Reproductive Glands Develop from Imaginal Precursors Marked by *lz* Expression

We initially investigated reproductive gland development at the cellular level using gene expression markers. With a *lz-Gal4* driven *UAS-GFP* transgene [32], *lz* expression was first detected in the genital imaginal disc about 0 hr after puparium formation (APF; see Figures S1A–S1C available online). Expression occurs within the four gland precursor domains, as evidenced by their location relative to *en* expression and by the protrusion of lz^+ cells at 8 hr APF (Figure 2A). The same expression pattern was seen using a specific anti-Lz antibody (Figures S1A–S1C), except that *lz-GAL4/UAS-GFP* expression, but not antibody staining, variegated. By contrast, no *lz* expression was seen in similarly aged male genital discs (data not shown), consistent with a recent report [20]. Thus, *lz* expression can be used to precisely mark early female reproductive gland precursor populations and to investigate how subsequent gland development takes place.

Two subpopulations of cells emerge within both SP and PO gland heads at about 24 hr APF when they become multilayered (Figure 2B). Many basally located cells lose *lz* expression beginning at 26 hr APF (Figure 2C). By 35 hr APF, individual lz^- cells ring the central part of the spermathecal head basally, whereas apical cells continue to express *lz* (Figure 2D). Cells around the top of the spermathecal head (where secretory cells do not form) and all duct cells remain lz^+. This suggests that the new lz^- cells correspond to secretory unit precursors (SUPs). By 48 hr, APF lz^- cells in both SPs and POs have become organized into three-cell clusters separated by lz^+ epithelial cells (Figure 2E). Luminal and ductal epithelial cells, but not secretory cells, express *lz* in adult female reproductive glands (Figure 2F), consistent with the idea that *lz* shuts off in secretory precursors.

Secretory Cell Progenitors Downregulate *lz* and Proliferate More than Other Gland Cells

We used a dual lineage tracing system [33] that marks ongoing *lz* expression (with RFP) and the lineal derivatives of all *lz*-expressing cells (with GFP) to confirm these conclusions (Figure 2G). GFP was detected in all reproductive gland cells, including secretory cells (Figure 2G″), but not in any other genital disc derivatives, which verified that lz^+ cells in the female genital disc give rise to all gland cells but to no other disc-derived parts of the reproductive tract. Only gland epithelial and ductal cells expressed RFP (Figure 2G). Thus, all female reproductive gland cells derive from lz^+ cells, but *lz* expression is downregulated in the secretory cell lineage.

Secretory cells were much more dependent on cell division than other gland cells. We used *lz-GAL4* to drive RNAi constructs that target the key cell-cycle genes *cycA*, *cdc2*, or *stg* to block cell proliferation (Figures S1D–S1F). The stunted SPs that resulted from knocking down either *cycA* or *cdc2* virtually lack secretory cells, but the dimensions of the lumen were only reduced by 25% and the ducts were only shortened by half (Figures S1G–S1I). Thus, secretory cell production entirely depends on precursor cell proliferation, whereas luminal and duct cell number is only augmented 2-fold or less after puparium formation.

Secretory Cells Differentiate as Part of Three-Cell Secretory Units with a Defined Cell Lineage

Detailed insight into post-larval divisions was obtained from further lineage analysis. A few cycling cells were marked randomly at specific times by transiently inducing FLP via a brief heat shock, and the daughters of these marked cells were mapped at various intervals thereafter (Figure 3A). The low labeling frequency of less than one clone per gland ensured that each cluster of labeled cells derived from a single progenitor. We categorized the clones in the gland head into SC or non-SC clones (containing or not containing a secretory cell respectively; Figure 3B). As expected from the results of blocking cell division, non-SC clones induced at 14 hr APF contained fewer than 1.5 cells on average and consisted of either one or two lz^+ epithelial cells adjacent to the lumen

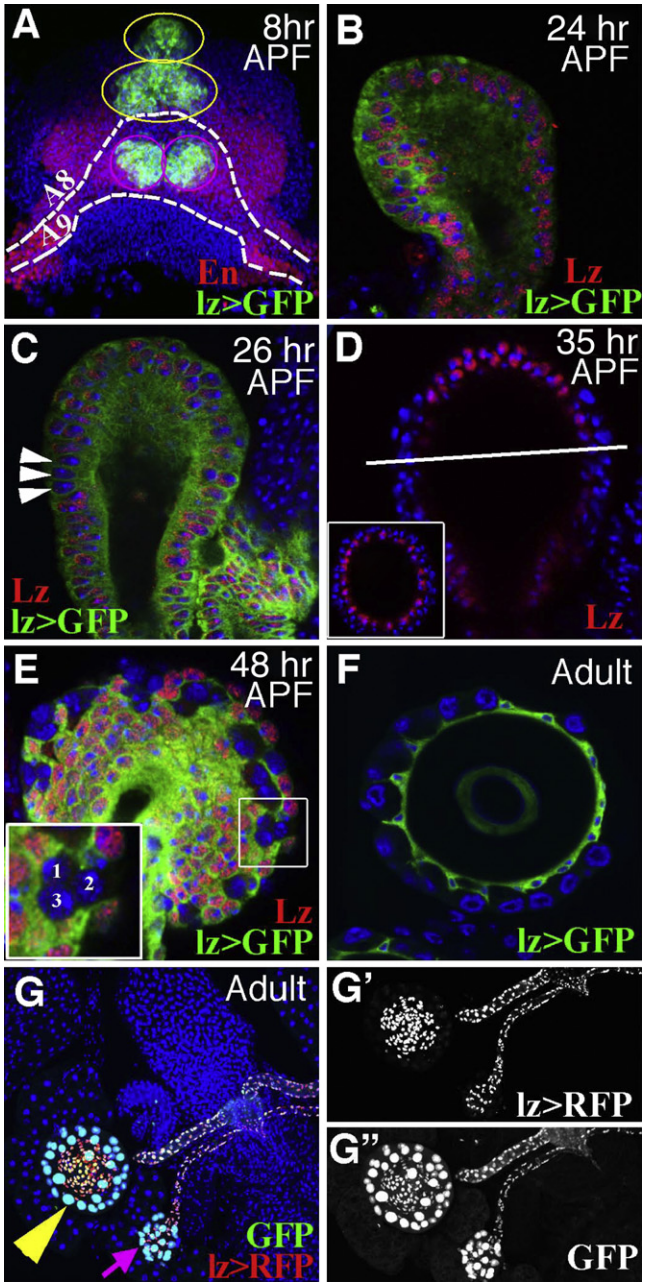

Figure 2. Reproductive Glands Originate from *lz*-Expressing Cells in the Female Genital Disc

(A) The dorsal view of a female genital disc at 8 hr APF showing En (red) and *lz* expression (green; *lz* > *GFP* = *lz-Gal4::UAS-GFP*) to reveal the four reproductive gland primordia (green cells). Precursors of the two SPs straddle the midline in the anterior and posterior regions of the A8 segment (yellow circles). PO precursors lie laterally off the midline within the posterior domain of the A9 segment (magenta circles).

(B and C) A sagittal section of spermathecal head with *lz* expression (green) and Lz antibody staining (red). Cells lacking Lz (arrowheads) arise basally between 24 and 26 hr APF.

(D) Cells at the top of the spermathecal head continue to express Lz (red) at 35 hr APF; sagittal section, inset: cross-section (white bar).

(E) By 48 hr APF, basal clusters each contain three lz^- cells (see inset).

(F) *lz* is expressed in epithelial cells but not SCs of adult SPs.

(G–G") Adult SP (yellow arrowhead) and PO (magenta arrow) epithelial and duct cells express *lz* (RFP in red), whereas lineage tracing (GFP, Experimental Procedures) shows that all SP and PO cells, including SCs, but not other cells of the female reproductive tract, derive from lz^+ progenitors.

(Figures 3B and 3C). Cells giving rise to such clones were termed "luminal epithelial precursors" (LEPs; Figure 3L). Clones of epithelial cells were only observed infrequently and contained just one cell when inductions were carried out at 24 hr and scored at 72 hr APF (abbreviated 24–72 hr), indicating that most LEPs cease dividing by 24 hr APF.

The behavior of SC clones was very different. In 14–72 hr clones, SC clones were larger and almost always consisted of exactly three lz^- cells (Figures 3C and 3D). These three-cell clones were highly structured and spatially ordered along the apical-basal axis. Usually, such clones have a small oval-shaped cell positioned adjacent to the lumen (the apical cell, AC). Next to the AC lies a large, polyploidy SC, whereas even more basally a third cell of intermediate size is present (the basal cell, BC; Figure 3D). Partner cells to the SC are lacking in adult glands. We verified the transient nature of ACs and BCs by further clonal analysis. In 24–72 hr clones, all SC clones contained a typical three-cell unit (Figure 3B). In 24–92 hr clones, the number of labeled cells decreased to two (Figure 3B), which always consisted of a SC and a BC (Figure 3E). However, 24 adult clones contained only a single cell, the SC (Figures 3B and 3F). These experiments precisely map the time of loss of both ACs (72–92 hr APF) and BCs (92 hr APF—one day of adulthood). Likewise, we determined the order of divisions giving rise to the three-cell units. In 31–72 hr clones, SC clones contained exactly two cells, one SC and one BC (Figure 3G). In addition, a new class of single-cell, nonluminal, non-SC clones was also observed, likely corresponding to single ACs (Figure 3B). In 42–72 hr clones, no multicellular clones were obtained. These observations indicate a precise lineage defined by an initial division of the SUP and a subsequent division of one of the daughters (pIIa; Figure 3L). No evidence for division of the second daughter (pIIb) was found even in 14–48 hr SC clones (Figures 3B and 3H).

We next analyzed earlier clones to investigate whether SUP and LEP specification is coordinated. In 8–72 hr clones, clones that mark cells upstream from the SUP fell into three categories (Figures 3I–3K). Clones of four or five cells contained a typical three-cell SC unit (from one SUP) plus one or two cells whose high β-galactosidase (β-gal) expression marked them as epithelial cells outside the secretory lineage (Figures 3I–3J). Thus, more than 70% of the time (n = 14), the precursor of the SUP undergoes a differential division resulting in a lz^+ LEP and a lz^- SUP (Figure 3L). However, the remaining cases consisted of six-cell clones made up of two typical three-cell SC-containing units (Figure 3K). Overall clone induction was too infrequent for these to be adjacent, independent three-cell clones. Thus, about 30% of the time, a symmetric division generates two daughter SUPs.

During SP formation in some insects, a cilium from one of the accessory cells is reported to participate in canal formation during secretory unit morphogenesis [34]. To investigate whether *Drosophila* secretory units transiently utilize cilia, we carried out an electron microscopic (EM) study of the forming secretory units. No evidence of cilia was observed (data not shown). Furthermore, secretory cells formed normally within flies in which the ciliary genes *unc* or *Pkd2* were knocked down using *actin-GAL4*-driven RNAi constructs (Figures S2A and S2B). The constructs were effective because males of

Blue represents DAPI staining of DNA in this and all subsequent figures. See also Figure S1.

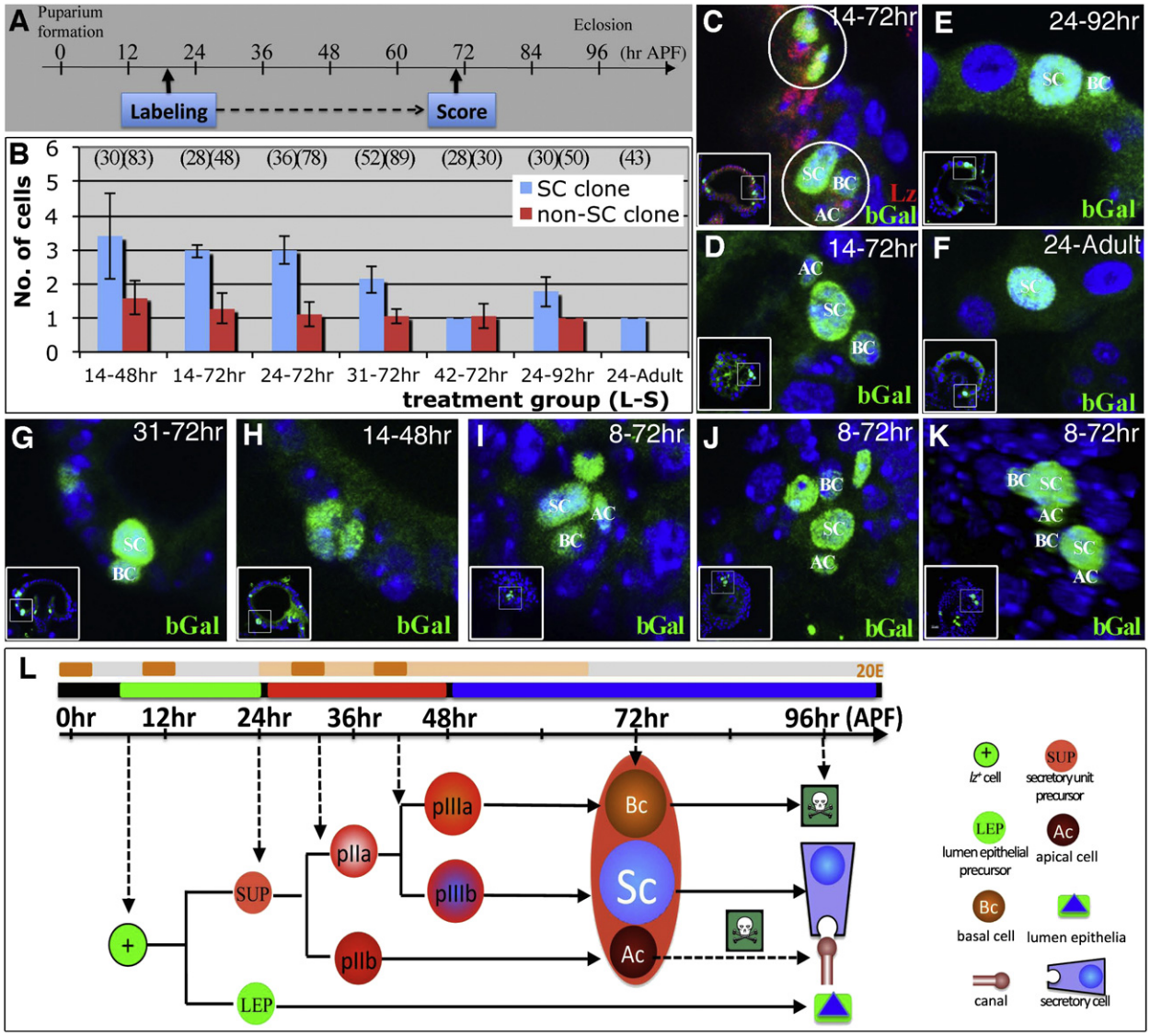

Figure 3. Lineage Analysis of Secretory Unit Formation

(A) Schematic lineage experiments in which marked clones were induced by heat shock ("labeling") and scored ("score") later in pupal development.

(B) Mean clone sizes in seven treatment groups. Each group is summarized on the x axis by "L-S," which indicates clone induction at time L and scoring at time S (in hr AFP). The average clone size is plotted (±SD) separately for SC (blue) and no-SC (red) clones. The number of clones analyzed is above in parentheses.

(C) An example of a SC (bottom circle) and a non-SC (upper circle) clone in 14–72 hr APF treatment group. Clone marker β-gal is in green and Lz staining in red. Note the Lz^+ cell in the bottom circle is β-gal-negative. AC, apical cell; BC, basal cell; SC, secretory cell. The boxed area in inset shows the clone location in the entire SP.

(D–K) Examples of SC clones from the indicated treatment groups following staining with β-gal (green).

(L) A model showing the lineage of female reproductive gland. Cell divisions are shown on a developmental timeline (top) in hours after puparium formation (APF). Times of major events: orange, ecdysone pulses; light orange, high ecdysone level; green, precursor protrusion, proliferation, and specification; red, secretory unit production; blue, secretory unit maturation. See also Figure S2.

the same genotype were sterile, like *unc* and *Pkd2* mutants [35–37].

Hr39 Functions Cell Autonomously in Gland and Secretory Cell Formation

The finding that secretory cells arise from lz^- precursors suggested that *Hr39* might regulate their development. A good anti-Hr39 antibody is lacking and it has been difficult to follow Hr39 RNA expression within pupal imaginal tissue. To obtain greater sensitivity, we analyzed pupal *Hr39-lacZ* expression using an anti-β-gal antibody that had been preabsorbed against control imaginal discs lacking a *lacZ* gene to remove background. No *Hr39* expression was detected in female genital discs from late larvae (Figure 4A). However, *Hr39-lacZ* expression is enriched in the spermathecal and parovarian domains defined by *lz-GAL4::UAS-GFP* expression at 8 hr and 20 hr APF (Figure 4B; Figure S3B). Lower level of expression was also detected in all other female genital disc cells (Figure 4B′) and within the male genital disc inner layer (Figure S3A). At 40 hr APF, *Hr39* continued to be expressed in all

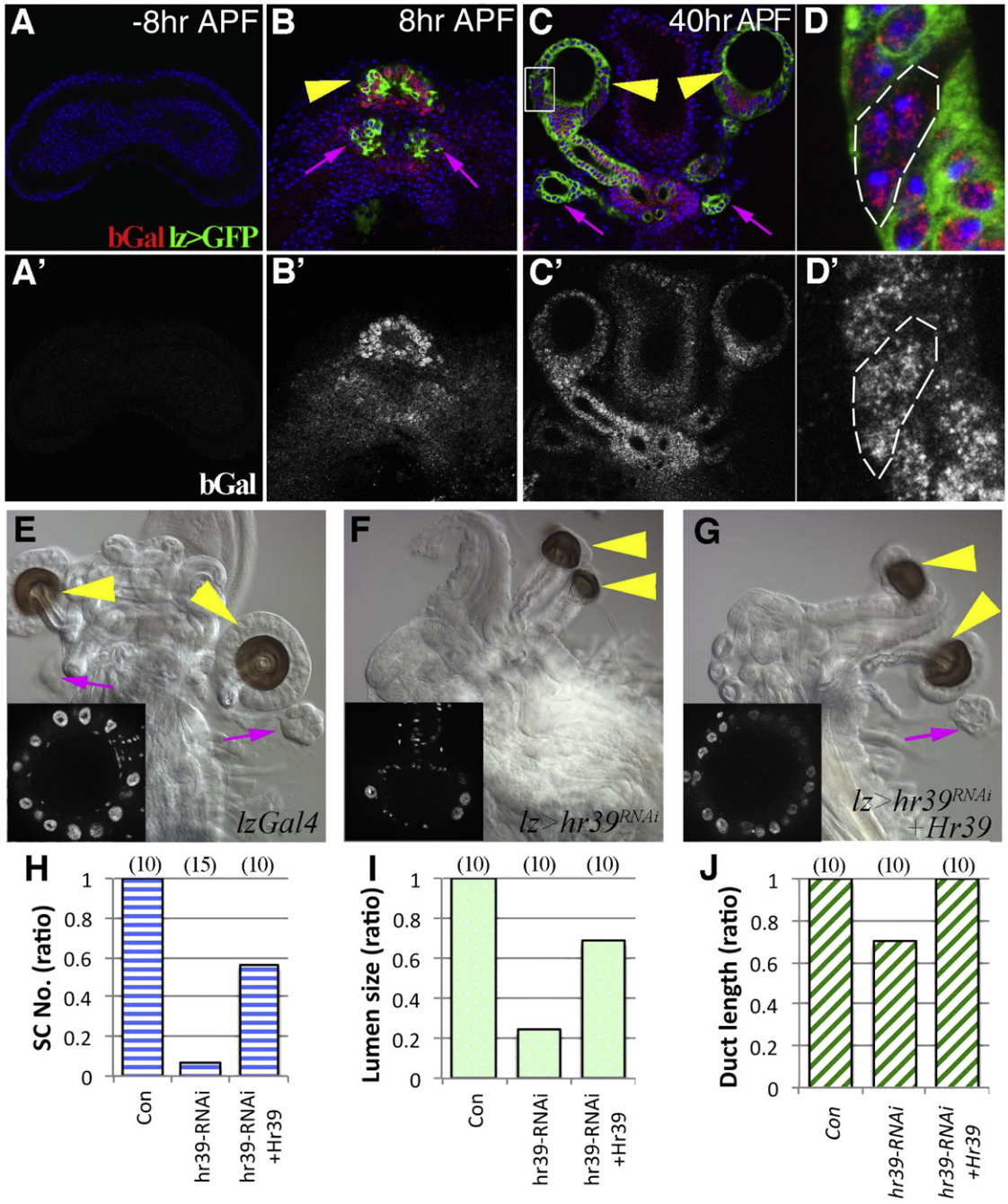

Figure 4. *Hr39* Is Expressed and Required in Gland Progenitor Cells

(A–D') *Hr39* transcription indicated by β-gal expression (red in A–D and white in A'–D') in female genital discs at −8 hr APF (A), 8 hr APF (B), or 40 hr APF (C and D) with one copy of the enhancer trap (*Hr39-lacZ*). *Hr39* transcription is highly enriched in the spermathecal (yellow arrowhead) and parovarian (magenta arrow) domains of genital discs at 8 hr APF and 40 hr APF. (D) is the higher magnification of boxed area in (C) showing a three-cell secretory unit with *Hr39* expression (without *lzGal4:: UASGFP*, outlined).

(E–G) DIC images showing adult female reproductive tract of *lz-Gal4* control (E), *Hr39* knockdown (F), and *Hr39* rescue (G) flies. Yellow arrowheads point to SP and magenta arrows point to PO. Inserts show the DAPI signal of the spermathecal head; the large bright DAPI signals are secretory cell nuclei.

(H–J) Quantification of SC number (H), lumen area size (I), and duct length (J) in SPs of different genotypes. *lz-Gal4* serves as a control. The number of females analyzed is in parentheses. See also Figure S3.

reproductive gland cells, including the developing secretory units (Figures 4C and 4D). Thus, unlike *lz*, *Hr39* expression is not shut off within the secretory lineage.

We depleted *Hr39* function via *lz-Gal4*-driven RNAi to investigate whether *Hr39* functions directly within gland precursor cells. Parovaria did not form at all, whereas spermathecae were altered in structure (Figures 4E and 4F). Secretory cells were absent, lumen size was reduced 5-fold, and duct length was about one third of normal (Figures 4H–4J). Thus, *Hr39* functions in early precursors of all gland cell types and is

strongly required in secretory cells. These defects were largely reversed by simultaneously expressing *Hr39* complementary DNA (cDNA) along with *Hr39* RNAi (Figure 4G), arguing that they represent specific *Hr39* functions.

The ability of mammalian NR5A genes to substitute for *Hr39* was also tested. Even in strong *Hr39* mutant females, 32% still retain one or both SP ducts, and the frequency of such ducts is readily quantified (Figures S3C and S3D). Duct formation in such animals was completely rescued by expressing *Hr39* cDNA; glands also formed but were frequently abnormal, most likely due to altered temporal expression (Figure S3E). When mouse *LRH-1* cDNA was driven by *lz-GAL4* in this background, SP duct formation was restored in more than 70% of females (Figures S3F and S3G). Small gland lumens formed occasionally and sometimes contained one or two SCs (Figure S3F). In contrast, expressing mouse *SF-1* cDNA using the same driver completely suppressed SP duct formation (Figure S3H).

Hr39 Is Required for Protrusion, Proliferation, and Survival of lz^+ Precursors during Early Pupation

We analyzed the behavior of reproductive gland precursors in *Hr39* mutant genital discs to better understand *Hr39* function. Patterning genes were expressed normally in *Hr39* mutant larval genital discs (Figure S4) and *lz*-expressing gland precursors were present in normal numbers (Figures 5A and 5B), confirming that *Hr39* neither patterns the disc nor establishes initial precursor pools. However, by 8 hr APF, *Hr39* mutant gland precursors protruded much less than control (Figure 5B). At 16 and 24 hr APF, wild-type (WT) but not *Hr39* mutant gland precursors had rounded up and protruded extensively (Figures 5C–5F). Moreover, the number of lz^+ precursors was clearly reduced in *Hr39* mutant discs by 16 hr (Figure 5G) in both the spermathecal and parovarian domains (Figure 5H).

We measured the frequency of cell division to verify that *Hr39* mutant gland precursors fail to proliferate. Staining of the M-phase marker phosphohistone H3 was readily detected at 9 hr APF in lz^+ precursors in control genital discs, but not in *Hr39* mutant discs (Figures 5I–5K). No apoptosis of lz^+ cells was observed in either control or *Hr39* mutant genital disc up to 16 hr APF (data not shown). However, by 20 hr APF, *Hr39* mutant (but not control) cells within both the anterior spermathecal domain and the two parovarian domains began to undergo apoptosis (Figures 5L and 5M). By 48 hr APF, all lz^+ cells had disappeared from these domains in *Hr39* mutants (data not shown). Therefore, *Hr39* is required for the protrusion, proliferation, and survival of reproductive gland precursors prior to the differentiation of secretory cells.

Ectopic *Hr39* Is Sufficient to Stimulate Protrusion and to Generate Spermatheca-like Structures in the Male Reproductive Tract

To test whether *Hr39* is sufficient to trigger gland formation, we examined clones of marked cells that misexpress *Hr39* in late larval imaginal discs. Interestingly, in contrast to control clones (Figures 6A–6C), *Hr39*-expressing clones in the wing, leg, eye-antennal, and genital discs developed a distinctive shape similar to early stages of gland protrusion (Figures 6D–6F; data not shown). Not only did the cells bulge out from the disc, but they frequently developed a central lumen (Figures 6D–6F). About 90% of clones in the wing, leg, and male genital disc clones protruded. About 28% of similarly sized clones in the female genital disc protruded, but none of the control clones did so (Figure 6G). By contrast, misexpression of *lz* in clones within these same tissues did not cause similar protrusion or lumen formation (Figures 6H and 6I). Unlike *Hr39*, *lz* misexpression was toxic and many cells died prior to pupation.

Hr39-misexpressing cells usually underwent apoptosis during pupal development. Clones in the wing, leg, and eye-antennal discs were never detected in corresponding adult structures. Surprisingly, however, a few clones induced in the male genital disc did survive and grow further. In three separate experiments, in which a total of 100 males were examined following clone induction, four examples of surviving adult clones were observed (Figure 6J). Two were located near the junction between the ejaculatory duct and penis, one was loosely attached to the ejaculatory duct, and the fourth clone was near the ejaculatory bulb. The surviving cells were organized in a round structure (Figure 6L), entirely different in appearance from control clones (Figure 6K). All four contained a central lumen covered by a brown-pigmented cell layer (Figure 6L″). Most strikingly, the clone at the ejaculatory bulb was connected to the bulb by a duct (Figure 6L″, arrow), and sperm were present inside the lumen, as revealed by DAPI staining (Figure 6L′, arrowheads). The ejaculatory bulb in this male also contained sperm, which is not normally observed. The shape, pigmentation, and sperm content of the *Hr39*-induced structures were characteristic of spermathecae. Thus, clonal ectopic *Hr39* expression in the male genital disc at low frequency generates a spermatheca-like structure in the male reproductive tract that when properly connected can attract and store sperm.

Discussion

The *Drosophila* Spermatheca as a Model Insect Gland

Our studies define the cellular events of reproductive gland formation and reveal that *lz* and *Hr39*, despite their nearly identical loss-of-function phenotypes, have distinctive expression patterns during gland development. All gland precursors express both genes following puparium formation, but within 24 hr divide to produce lz^+ epithelial precursors apically and lz^- SUPs basally. SUPs then differentiate according to a stereotyped program involving production of two transient accessory cells and a single polyploid secretory cell.

Our studies show that reproductive secretory cells arise in a superficially similar manner to sensory bristles and multiple classes of mechanosensory and chemosensory sensilla [38]. Both utilize short fixed-cell lineages that employ transient accessory cells to generate permanent extracellular structures (secretory canal, sensory bristle, etc.), but the three-cell secretory lineage analyzed here differs from the four asymmetric divisions producing five different cells typical of PNS differentiation [39]. Many other insect epidermal glands probably develop in a generally similar manner, but the precise cell lineages and mechanisms documented here for *Drosophila* reproductive glands (three cells, absence of ciliary involvement) differ from previous models [15].

Drosophila secretory units provide a powerful system for analyzing insect gland development. Studies in other insects suggested that an accessory cell utilizes a ciliary process to prevent the SCs from being sealed off by cuticle-secreting epithelial cells [14, 16, 34]. We found no morphological or genetic evidence that cilia are involved in forming *Drosophila* secretory units (Figures S2A and S2B). However, the AC may fulfill this same role using normal microtubules, in much the

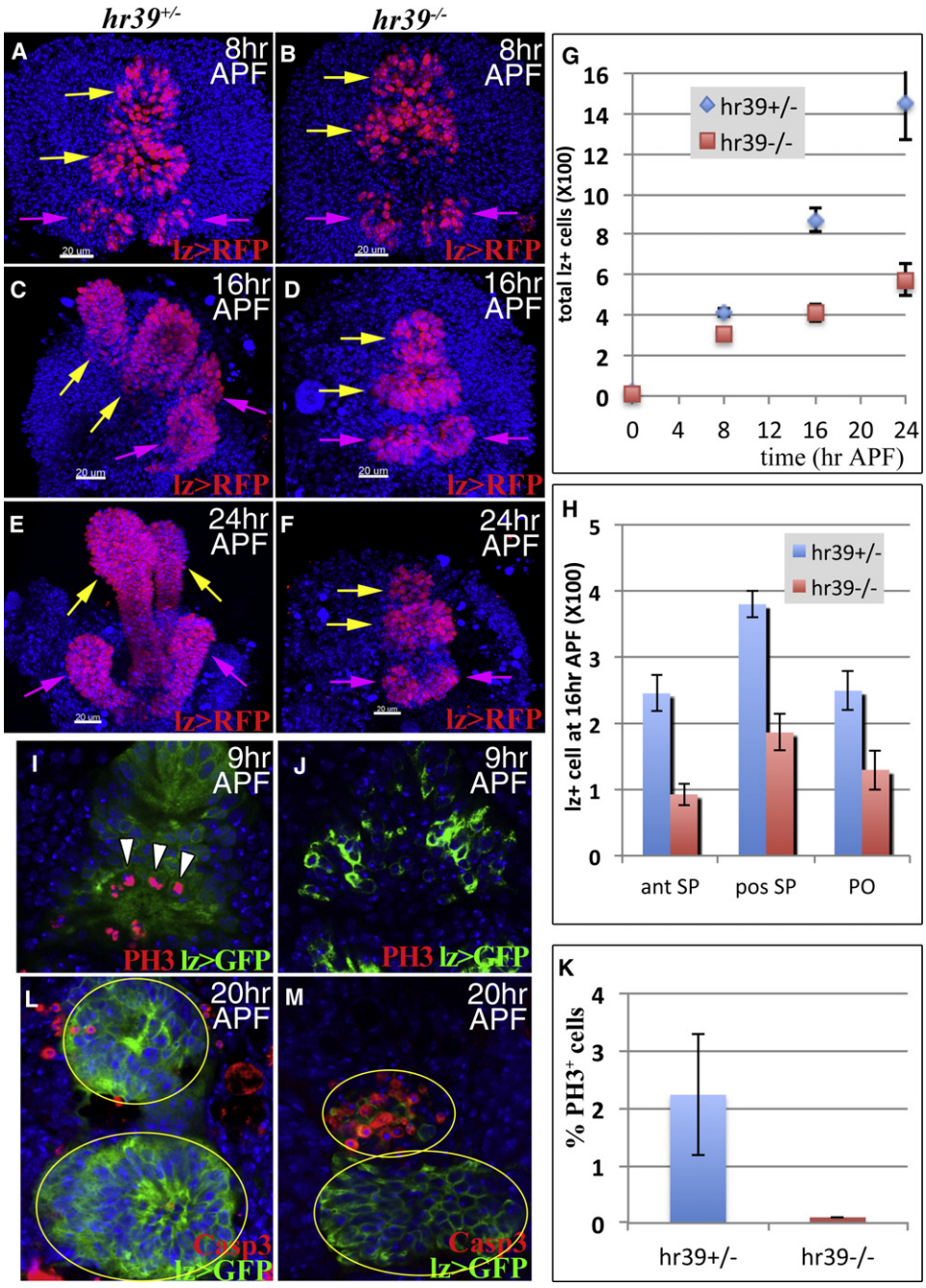

Figure 5. *Hr39* Mediates the Protrusion, Proliferation, and Survival of Gland Precursors

(A–F) The dorsal-lateral view of female genital discs showing cells expressing *lz* (*lz > RFP = lzGal4::UAS-nlsRFP*) in pupal genital discs at the indicated times from control (A, C, and E) and *Hr39* mutant (B, D, and F) females. SP (yellow arrows) and PO (magenta arrows) primordia are indicated. The scale bar represents 20 μm.

(G) The average number of total lz^+ cell in female genital discs at different times is plotted. Cells from five animals for each genotype at each time point were counted. Error bar represents SD.

(H) The number of lz^+ cells in anterior (ant) and posterior (pos) SPs and PO domains at 16 hr APF is plotted.

(I–K) Dividing cells were labeled using phosphohistone H3 (PH3) staining (red) in control (I) or *Hr39* mutant (J) genital discs and the percentage of $PH3^+$ cells in lz^+ cell group is plotted in (K).

(L and M) Apoptotic cells were labeled using active Caspase 3 staining (Casp3, red) in control (L) and *Hr39* mutant (M) genital discs at 20 hr APF. See also Figure S4.

same way that the anterior polar cells in egg chambers template the micropyle channel during oogenesis [40]. Membranes from the BC likely surround this AC process, secrete the cuticular canal, and join it to the luminal cuticle. Concomitantly, the BC likely secretes the end apparatus around a large apical segment of the SC, which it surrounds.

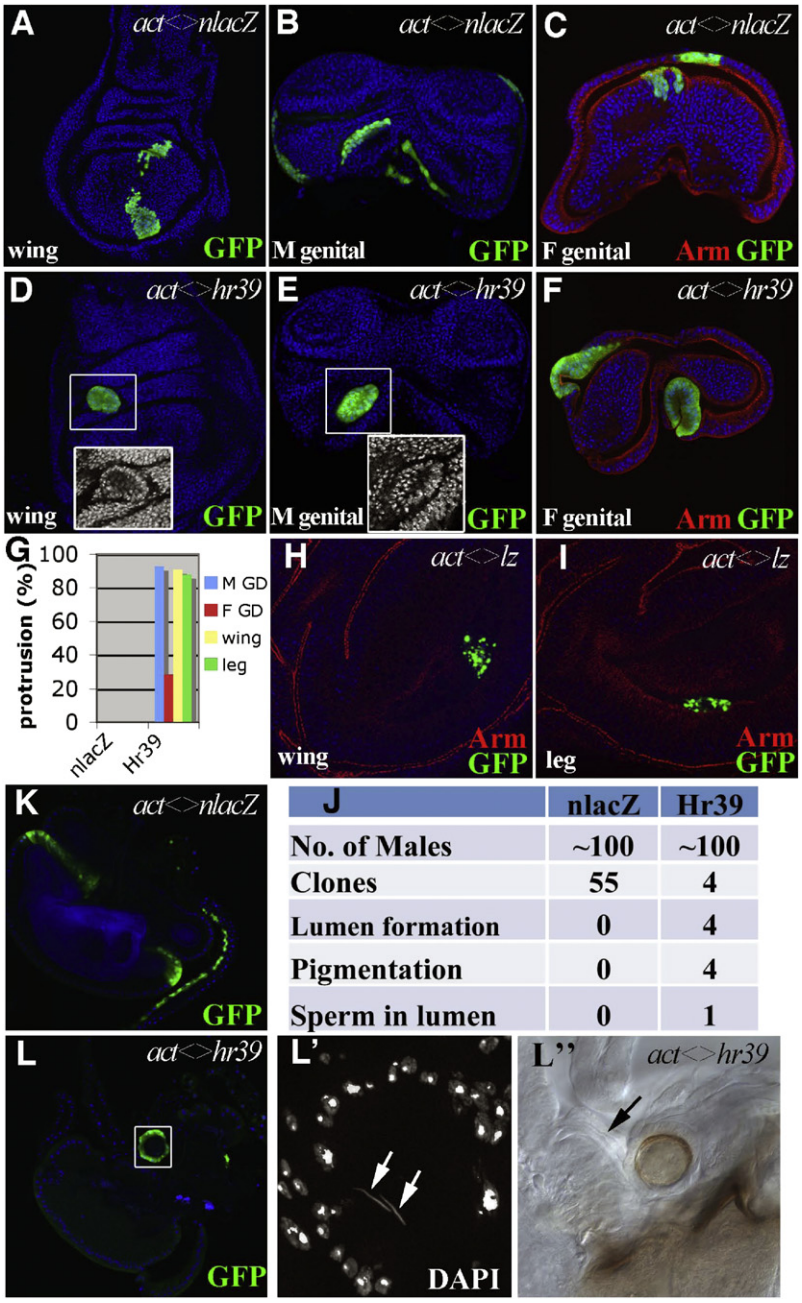

J	nlacZ	Hr39
No. of Males	~100	~100
Clones	55	4
Lumen formation	0	4
Pigmentation	0	4
Sperm in lumen	0	1

Figure 6. *Hr39* Misexpression Induces Protrusion and Ectopic Spermatheca Formation

(A–F) Morphology of flip-out clones (marked by GFP) expressing nlacZ (A–C) or Hr39 (D–F) in wing (A and D), male (B and E) and female (C and F) genital discs at the late third-instar larval stage. Armadillo (Arm, red) highlights the apical side of the epithelia. Insets show higher magnification of DAPI signal in the boxed area.

(G) Quantification of protruding clones of control and Hr39-misexpressing imaginal discs. About 30–60 clones were analyzed in each disc.

(H and I) Cells misexpressing Lz show apoptosis with fragmented GFP signals in wing (H) and leg (I) discs of third-instar larvae.

(J) A summary of phenotypes of the Hr39-misexpressing clones in the adult male reproductive tract.

(K) Control clones in adult male reproductive tract. Clones are in the ejaculatory bulb and duct.

(L–L'') A Hr39-expressing clone in the male ejaculatory bulb shows a circular shape with a lumen in the center. (L') shows a higher magnification of the DAPI signal in the boxed area to highlight sperm nuclei (arrows) in the lumen. The lumen has brown pigmentation (DIC image in L'') with a tiny duct (arrow) connected to the ejaculatory bulb.

Hr39 Regulates Gland and Secretory Cell Development at Multiple Levels

The NR5A hormone receptor Hr39 plays multiple roles in reproductive gland development. Initially, Hr39 orchestrates gland protrusion and in the absence of Hr39 protrusion fails to occur. Among *Drosophila* imaginal discs, gland protrusion in genital discs is a unique process that leads to the differentiation of a gland capsule connected to the nascent reproductive tract by a tubular duct. When *Hr39* is misexpressed, patches of cells within multiple imaginal discs that do not normally express *Hr39* undergo changes reminiscent of early protrusion.

Hr39, a known member of the ecdysone response pathway [41], is likely to time reproductive gland cell divisions during pupal development. The initial *Hr39* expression we observed in the genital disc was detected shortly after the prepupal ecdysone pulse. Several additional peaks of ecdysone titer during pupal development [42] correspond closely with the timing we measured of the secretory cell divisions. These observations suggest that external hormonal signals rather than internal autonomous mechanisms sometimes drive precise cell lineages. In addition to its requirement within cellular precursors, *Hr39* mutations alter SP secretory gene mRNA levels [5], suggesting that *Hr39* also regulates secretory gene expression within SCs.

Finally, Hr39 acts as a high level "master regulator" by integrating individual pathways to elicit the production of an entire gland. Most cells expressing ectopic *Hr39* could not progress past the initial stage of eversion, but in male genital discs *Hr39*-positive clones sometimes generated integrated structures that strongly resembled small spermathecae. They contained round heads with lumens, a pigmented layer, and rarely were connected to the male reproductive tract by ducts through which sperm were taken up (Figure 6L). Thus, *Hr39* (but not *lz*) can reprogram male genital cells to generate ectopic spermathecae that likely synthesize and secrete products attractive to sperm.

Female Reproductive Glands Differentiate from Developmentally Sensitive Precursor Pools

Drosophila reproductive gland development is unusually susceptible to perturbation. Rare adults in some wild strains contain an extra spermatheca, and females bearing weak alleles of either *lz* or *Hr39* lose POs entirely and produce fewer SPs, which vary dramatically in size and cellular content [5, 19]. These effects probably result from the disparate sizes of the precursor pools for individual organs (Figure 5). PO pools are very small, whereas the exceptionally large posterior SP

primordium may easily split in two under conditions where precursor proliferation is perturbed. The effects of *dac* mutations on duct structure [22] are probably also due to altered precursor pools. Sphingolipids may affect gland development [25] by serving as endogenous Hr39 ligands, consistent with reports that SF-1 can bind sphingolipids [41, 43].

Development and Function of Female Reproductive Glands May Be Conserved

In mammals, sperm interact with female secretory products at multiple locations. Glands within the uterine endometrium are hypothesized to govern selective passage through the cervix, uterus, and subsequently, the uterotubal junction [4]. Following entry into the oviduct, sperm induce and interact with the products of specialized tubal secretory cells that likely mediate capacitation [44]. In some species, these products also allow sperm to be stored in the oviduct while retaining their ability to fertilize an egg [4]. Mammalian female reproductive glands continue to nurture preimplantation embryos and are likely essential for successful pregnancy [45].

Drosophila is emerging as a valuable model with which to study multiple aspects of reproductive physiology, some of which may have been conserved during evolution [3, 5–7]. The mouse *lz* homolog *Aml1 (Runx1)* is expressed in the Müllerian ducts and genital tubercle [46], but its role in fertility is unknown. The murine *Hr39* homolog *LRH-1* is required for female fertility [26], but whether it plays a role in reproductive gland secretion has yet to be tested. However, LRH-1 is required for the development of several exocrine tissues [47] and in the pancreas is directly involved in the transcription of major secretory products [31]. Thus, *LRH-1* and *Hr39* may both govern the formation and secretory function of exocrine tissue.

Our studies provide further support for the idea that an NR5a-dependent program of secretory cell development has been conserved in evolution. Murine LRH-1 can partially replace Hr39 function in *Drosophila* reproductive gland formation. Similar rescue with two other NR5A members (mammalian SF-1 or *Drosophila* Ftz-F1) failed and instead suppressed all gland formation (Figures S3F–S3H; data not shown). This is consistent with previous findings that Hr39 and Ftz-F1 have opposing roles in alcohol dehydrogenase and EcR expression [48, 49]. Antagonistic roles in gene regulation by the two NR5A family members may be evolutionarily conserved. Further study of the roles of Hr39 and LRH-1 should help define a fundamental program of secretory cell development that may be widely used.

Experimental Procedures

Drosophila Genetics

Drosophila were reared on standard cornmeal-molasses food at 25°C unless otherwise indicated. White prepupae (designated as 0 hr APF) were collected over a 30 min period and aged to the desired stage. All stocks not otherwise indicated were from the Bloomington Drosophila Stock Center. *UAS-mCD8:GFP*, *lz-Gal4*, and *lz-Gal4;UAS-GFP* stocks [32] were used to map *lz* expression in genital discs by staining with anti-GFP antibodies. *lz-Gal4*-bearing flies were crossed to *UAS-RedStinger, UAS-FLP, ubi<Stop< Stinger* to monitor real-time expression and lineage expression of *lz* [33]. Clonal labeling was initiated by heat shocking (37°C, 60 min) pupae of genotype *hsFLP; X-15-29/X-15-33* [50]. RNAi lines targeting *cyclin A* (V32421), *cdc2* (V41838), *stg* (V17760), and *Hr39* (V37694) were obtained from the Vienna Drosophila RNAi Center and used at 29°C. $Hr39^{07154}$, a strong loss-of-function allele caused by a lacZ enhancer trap insertion [5], was used to map *Hr39* expression and is designated *Hr39-lacZ*. Unless otherwise denoted, *Hr39* mutant animals were $Hr39^{07154}$ homozygotes.

For clonal misexpression, *hsFLP; act<CD2<Gal4, UAS-GFP* [51] flies were crossed to either *UAS-nlacZ* or *UAS-Hr39* [5]. To induce such clones, we heat-shocked embryos aged from 16 hr to 24 hr after egg laying for 45 min in a 37°C water bath. For rescue experiments, *UAS-mCD8:GFP, lz-Gal4;* $Hr39^{07154}$*/CyO* flies were crossed to (1) $Hr39^{07154}$*/CyO*, (2) $Hr39^{07154}$*/CyO;UAS-Hr39*, (3) $Hr39^{07154}$*/CyO;UAS-mLRH-1* (a generous gift from Leslie Pick), or (4) $Hr39^{07154}$*/CyO;UAS-mSF-1* [52].

Immunostaining and Microscopy

Larval and pupal imaginal discs and adult reproductive tracts were dissected in cold Grace's medium, then fixed in 4% formaldehyde + 0.2% Triton X-100 for 20 min at room temperature. Tissues were vigorously shaken after fixation to loosen attached fat tissues, blocked in antibody buffer (PBS+ 0.3% Triton X-100 + 0.5% BSA+ 2% normal goat serum), and stained with primary antibodies overnight at 4°C followed by secondary antibody staining. Chicken anti-β-gal antibody and all secondary antibodies were preabsorbed to minimize background. Primary antibodies used: mouse anti-En (1:20), anti-Lz (1:15), anti-Arm (1:40), anti-Wg (1:30), and anti-Dac (1:20) from Developmental Studies Hybridoma Bank; mouse anti-GFP (1:2,000, Invitrogen), anti-phospho-H3 Ser10 (1:1,000, Cell Signaling Technology); rabbit anti-GFP (1:4,000, Invitrogen), anti-RFP (1:1,000, MBL international), anti-cleaved Caspase 3 (1:100, Cell Signaling Technology); and chicken anti-β-gal (1:1,000, Abcam). The secondary antibodies were Alexa 488 or 568 goat anti-mouse, anti-rabbit, and anti-chicken antibodies (1:1,000, Invitrogen). DAPI staining was at 5 μg/ml for 10 min. All fluorescent images were acquired on a Leica TCS SP5 confocal microscope and differential interference contrast (DIC) images on a Zeiss Axioimager ZI microscope. Images were assembled using Imaris 3D software, ImageJ, and Photoshop.

Quantitation of Spermathecal Cell Number

Adult SCs within SPs were identified based on their elevated ploidy and distinctive nuclear morphology and manually counted. Adult luminal or ductal epithelial cell numbers were estimated from the gland luminal area or duct length, respectively, based on a constant ratio of cells per unit area or length that was determined empirically. The total duct length and lumen area was calculated by using ImageJ software to acquire the maximal projection of the z series of DIC images. The number of lz^+ cells in genital discs at particular pupal stages was determined using Imaris 3D software. lz^+ cells within the anterior SP, posterior SP, or POs were distinguished using position filters and manual examination.

Supplemental Information

Supplemental Information includes four figures and can be found with this article online at doi:10.1016/j.cub.2012.03.059.

Acknowledgments

We thank Bruce Baker and Audrey Christiansen for helpful discussion on genital disc development and *lzGal4* expression; Leslie Pick for sending flies with *UAS-mSF-1* and *UAS-mLRH-1* constructs; Utpal Banerjee for sending *lz* alleles and sharing information about Lz antibody staining; Mike Sepanski for the EM study of the developmental secretory unit; Don Fox for technical discussion on pupal dissection; and Becky Frederick, Ming-Chia Lee, Robert Levis, Vicki Losick, and Matt Sieber for comments on the manuscript. A.C.S. is an Investigator of the Howard Hughes Medical Institute.

Received: March 6, 2012
Revised: March 11, 2012
Accepted: March 13, 2012
Published online: May 3, 2012

References

1. Avila, F.W., Sirot, L.K., LaFlamme, B.A., Rubinstein, C.D., and Wolfner, M.F. (2011). Insect seminal fluid proteins: identification and function. Annu. Rev. Entomol. *56*, 21–40.
2. Chang, M.C. (1984). The meaning of sperm capacitation. A historical perspective. J. Androl. *5*, 45–50.
3. Bloch Qazi, M.C., Heifetz, Y., and Wolfner, M.F. (2003). The developments between gametogenesis and fertilization: ovulation and female sperm storage in Drosophila melanogaster. Dev. Biol. *256*, 195–211.
4. Holt, W.V., and Fazeli, A. (2010). The oviduct as a complex mediator of mammalian sperm function and selection. Mol. Reprod. Dev. *77*, 934–943.

5. Allen, A.K., and Spradling, A.C. (2008). The Sf1-related nuclear hormone receptor Hr39 regulates Drosophila female reproductive tract development and function. Development *135*, 311–321.
6. Manier, M.K., Belote, J.M., Berben, K.S., Novikov, D., Stuart, W.T., and Pitnick, S. (2010). Resolving mechanisms of competitive fertilization success in Drosophila melanogaster. Science *328*, 354–357.
7. Heifetz, Y., and Rivlin, P.K. (2010). Beyond the mouse model: using Drosophila as a model for sperm interaction with the female reproductive tract. Theriogenology *73*, 723–739.
8. Arbeitman, M.N., Fleming, A.A., Siegal, M.L., Null, B.H., and Baker, B.S. (2004). A genomic analysis of Drosophila somatic sexual differentiation and its regulation. Development *131*, 2007–2021.
9. Lawniczak, M.K., and Begun, D.J. (2007). Molecular population genetics of female-expressed mating-induced serine proteases in Drosophila melanogaster. Mol. Biol. Evol. *24*, 1944–1951.
10. Prokupek, A.M., Kachman, S.D., Ladunga, I., and Harshman, L.G. (2009). Transcriptional profiling of the sperm storage organs of Drosophila melanogaster. Insect Mol. Biol. *18*, 465–475.
11. Keisman, E.L., Christiansen, A.E., and Baker, B.S. (2001). The sex determination gene doublesex regulates the A/P organizer to direct sex-specific patterns of growth in the Drosophila genital imaginal disc. Dev. Cell *1*, 215–225.
12. Epper, F. (1983). The Evagination of the Genital Imaginal Discs of *Drosophila melanogaster* I. Morphogenesis of the Female Genital Disc. Rouxs Arch. Dev. Biol. *192*, 275–279.
13. Filosi, M., and Perotti, M.E. (1975). Fine structure of the spermatheca of Drosophila melanogaster Meig. J. Submicrosc. Cytol. *7*, 259–270.
14. Lococo, D., and Huebner, E. (1980). The development of the female accessory gland in the insect Rhodnius prolixus. Tissue Cell *12*, 795–813.
15. Noirot, C., and Quennedey, A. (1974). Fine structure of insect epidermal glands. Annu. Rev. Entomol. *19*, 61–80.
16. Büning, J. (1994). The Insect Ovary (London: Chapman and Hall), pp. 400.
17. Estrada, B., Casares, F., and Sánchez-Herrero, E. (2003). Development of the genitalia in Drosophila melanogaster. Differentiation *71*, 299–310.
18. Chen, E.H., Christiansen, A.E., and Baker, B.S. (2005). Allocation and specification of the genital disc precursor cells in Drosophila. Dev. Biol. *281*, 270–285.
19. Anderson, R.C. (1945). A Study of the Factors Affecting Fertility of Lozenge Females of Drosophila Melanogaster. Genetics *30*, 280–296.
20. Chatterjee, S.S., Uppendahl, L.D., Chowdhury, M.A., Ip, P.L., and Siegal, M.L. (2011). The female-specific doublesex isoform regulates pleiotropic transcription factors to pattern genital development in Drosophila. Development *138*, 1099–1109.
21. Canon, J., and Banerjee, U. (2000). Runt and Lozenge function in Drosophila development. Semin. Cell Dev. Biol. *11*, 327–336.
22. Keisman, E.L., and Baker, B.S. (2001). The Drosophila sex determination hierarchy modulates wingless and decapentaplegic signaling to deploy dachshund sex-specifically in the genital imaginal disc. Development *128*, 1643–1656.
23. Phan, V.H., Herr, D.R., Panton, D., Fyrst, H., Saba, J.D., and Harris, G.L. (2007). Disruption of sphingolipid metabolism elicits apoptosis-associated reproductive defects in Drosophila. Dev. Biol. *309*, 329–341.
24. King-Jones, K., and Thummel, C.S. (2005). Nuclear receptors—a perspective from Drosophila. Nat. Rev. Genet. *6*, 311–323.
25. Schimmer, B.P., and White, P.C. (2010). Minireview: steroidogenic factor 1: its roles in differentiation, development, and disease. Mol. Endocrinol. *24*, 1322–1337.
26. Duggavathi, R., Volle, D.H., Mataki, C., Antal, M.C., Messaddeq, N., Auwerx, J., Murphy, B.D., and Schoonjans, K. (2008). Liver receptor homolog 1 is essential for ovulation. Genes Dev. *22*, 1871–1876.
27. Guo, G., and Smith, A. (2010). A genome-wide screen in EpiSCs identifies Nr5a nuclear receptors as potent inducers of ground state pluripotency. Development *137*, 3185–3192.
28. Heng, J.C., Feng, B., Han, J., Jiang, J., Kraus, P., Ng, J.H., Orlov, Y.L., Huss, M., Yang, L., Lufkin, T., et al. (2010). The nuclear receptor Nr5a2 can replace Oct4 in the reprogramming of murine somatic cells to pluripotent cells. Cell Stem Cell *6*, 167–174.
29. Lee, J.M., Lee, Y.K., Mamrosh, J.L., Busby, S.A., Griffin, P.R., Pathak, M.C., Ortlund, E.A., and Moore, D.D. (2011). A nuclear-receptor-dependent phosphatidylcholine pathway with antidiabetic effects. Nature *474*, 506–510.
30. Lee, Y.K., and Moore, D.D. (2008). Liver receptor homolog-1, an emerging metabolic modulator. Front. Biosci. *13*, 5950–5958.
31. Holmstrom, S.R., Deering, T., Swift, G.H., Poelwijk, F.J., Mangelsdorf, D.J., Kliewer, S.A., and MacDonald, R.J. (2011). LRH-1 and PTF1-L coregulate an exocrine pancreas-specific transcriptional network for digestive function. Genes Dev. *25*, 1674–1679.
32. Crew, J.R., Batterham, P., and Pollock, J.A. (1997). Developing compound eye in lozenge mutants of Drosophila: lozenge expression in the R7 equivalence group. Dev. Genes Evol. *206*, 481–493.
33. Evans, C.J., Olson, J.M., Ngo, K.T., Kim, E., Lee, N.E., Kuoy, E., Patananan, A.N., Sitz, D., Tran, P., Do, M.T., et al. (2009). G-TRACE: rapid Gal4-based cell lineage analysis in Drosophila. Nat. Methods *6*, 603–605.
34. Sreng, L., and Quennedey, A. (1976). Role of a temporary ciliary structure in the morphogenesis of insect glands. An electron microscope study of the tergal glands of male Blattella germanica L. (Dictyoptera, Blattellidae). J. Ultrastruct. Res. *56*, 78–95.
35. Baker, J.D., Adhikarakunnathu, S., and Kernan, M.J. (2004). Mechanosensory-defective, male-sterile unc mutants identify a novel basal body protein required for ciliogenesis in Drosophila. Development *131*, 3411–3422.
36. Gao, Z., Ruden, D.M., and Lu, X. (2003). PKD2 cation channel is required for directional sperm movement and male fertility. Curr. Biol. *13*, 2175–2178.
37. Watnick, T.J., Jin, Y., Matunis, E., Kernan, M.J., and Montell, C. (2003). A flagellar polycystin-2 homolog required for male fertility in Drosophila. Curr. Biol. *13*, 2179–2184.
38. Lai, E.C., and Orgogozo, V. (2004). A hidden program in Drosophila peripheral neurogenesis revealed: fundamental principles underlying sensory organ diversity. Dev. Biol. *269*, 1–17.
39. Orgogozo, V., Schweisguth, F., and Bellaïche, Y. (2001). Lineage, cell polarity and inscuteable function in the peripheral nervous system of the Drosophila embryo. Development *128*, 631–643.
40. Montell, D.J., Rorth, P., and Spradling, A.C. (1992). slow border cells, a locus required for a developmentally regulated cell migration during oogenesis, encodes Drosophila C/EBP. Cell *71*, 51–62.
41. Urs, A.N., Dammer, E., Kelly, S., Wang, E., Merrill, A.H., Jr., and Sewer, M.B. (2007). Steroidogenic factor-1 is a sphingolipid binding protein. Mol. Cell. Endocrinol. *265-266*, 174–178.
42. Handler, A.M. (1982). Ecdysteroid titers during pupal and adult development in Drosophila melanogaster. Dev. Biol. *93*, 73–82.
43. Urs, A.N., Dammer, E., and Sewer, M.B. (2006). Sphingosine regulates the transcription of CYP17 by binding to steroidogenic factor-1. Endocrinology *147*, 5249–5258.
44. Georgiou, A.S., Snijders, A.P., Sostaric, E., Aflatoonian, R., Vazquez, J.L., Vazquez, J.M., Roca, J., Martinez, E.A., Wright, P.C., and Fazeli, A. (2007). Modulation of the oviductal environment by gametes. J. Proteome Res. *6*, 4656–4666.
45. Dunlap, K.A., Filant, J., Hayashi, K., Rucker, E.B., 3rd, Song, G., Deng, J.M., Behringer, R.R., DeMayo, F.J., Lydon, J., Jeong, J.W., and Spencer, T.E. (2011). Postnatal deletion of Wnt7a inhibits uterine gland morphogenesis and compromises adult fertility in mice. Biol. Reprod. *85*, 386–396.
46. Simeone, A., Daga, A., and Calabi, F. (1995). Expression of runt in the mouse embryo. Dev. Dyn. *203*, 61–70.
47. Fayard, E., Auwerx, J., and Schoonjans, K. (2004). LRH-1: an orphan nuclear receptor involved in development, metabolism and steroidogenesis. Trends Cell Biol. *14*, 250–260.
48. Boulanger, A., Clouet-Redt, C., Farge, M., Flandre, A., Guignard, T., Fernando, C., Juge, F., and Dura, J.M. (2011). ftz-f1 and Hr39 opposing roles on EcR expression during Drosophila mushroom body neuron remodeling. Nat. Neurosci. *14*, 37–44.
49. Ayer, S., Walker, N., Mosammaparast, M., Nelson, J.P., Shilo, B.Z., and Benyajati, C. (1993). Activation and repression of Drosophila alcohol dehydrogenase distal transcription by two steroid hormone receptor superfamily members binding to a common response element. Nucleic Acids Res. *21*, 1619–1627.
50. Harrison, D.A., and Perrimon, N. (1993). Simple and efficient generation of marked clones in Drosophila. Curr. Biol. *3*, 424–433.
51. Sun, J., and Deng, W.M. (2005). Notch-dependent downregulation of the homeodomain gene cut is required for the mitotic cycle/endocycle switch and cell differentiation in Drosophila follicle cells. Development *132*, 4299–4308.
52. Yussa, M., Löhr, U., Su, K., and Pick, L. (2001). The nuclear receptor Ftz-F1 and homeodomain protein Ftz interact through evolutionarily conserved protein domains. Mech. Dev. *107*, 39–53.